Table of Contents

Materials and Methods:

All starting materials for DNA synthesis were purchased from Glen Research (Sterling, USA) and Cambridge Isotope Laboratory (CIL, UK). Trimethylammonium acetate (TMAA, 1M stock solution) and potassium chloride (KCl, Bio Ultra) were purchased from Santa Cruz Biotechnology (Texas, USA) and Sigma-Aldrich (Saint-Quentin Fallavier, France). Unless otherwise specified, all other reagents/chemicals were purchased from MERCK (France).

All DNA samples for NMR experiments (unlabeled and site-specifically 4-8% ^{13}C and ^{15}N-labeled) were synthesized on K&A Laborgeraete GbR DNA / RNA synthesizer H-8 using standard Phosphoramidite chemistry in DMT off mode. After synthesis, the samples were deprotected in ammonium hydroxide solution (pH >8) for 16-18 hours and further treated with 2M LiCl before removing excess ammonia. Finally, the samples were desalted with an amicon-15 centrifuge filter (3 kDa cutoff) and lyophilized. After lyophilization, the oligonucleotides were dissolved in Milli-Q water. The concentration of stock solutions were calculated by measuring the absorbance at 260 nm in the Varian CARY-100 BIO UV–VIS instrument, assuming ε_{260} = 236500 $L \times M^{-1} \times cm^{-1}$ for all variants of the 23TAG sequence. For all the CD and ESI-MS experiments samples were purchased from Eurogentec (Seraing, Belgium) and dissolved in nuclease-free grade water from Ambion (Ambion, Life Technologies SAS, Saint-Aubin, France) to make samples at ~500 µM DNA concentration, which were stored at -20 °C.

Phen-DC_3 ligand was synthesized as previously described in powder form and dissolved in 99.96% Dimethyl sulfoxide-d_6 (DMSO-d_6) (CIL, UK) with a stock concentration of 20 mM determined from the absorbance (ε_{335} =14900 $L \times M^{-1} \times cm^{-1}$).[1] The stock solution was stored in several aliquots at -20 °C and was used as required.

Samples were prepared from DNA stock solution by firstly heating them at 95 °C for 2-3 minutes, immediately supplementing the solution with KCl and potassium phosphate (pH 7.0, NMR, CD buffer); KCl and TMAA (pH 7.0, ESI-MS buffer) or NaCl and Tris–HCl (pH 7.5) followed by slow cooling from 95 °C to 25 °C for 48 hours. For all NMR, ESI-MS, and CD experiments samples comprising aqueous solution of DNA were titrated with adequate aliquots of ligand (Phen-DC_3) and kept at room temperature (25 °C) for 48 hours before measurement.

Experimental Section

Circular Dichroism (CD) Spectroscopy

The CD spectra were recorded on a Jasco J-815 spectropolarimeter equipped with a JASCO CDF 426S Peltier temperature controller using a quartz cuvette (2 mm path length). The CD spectra were acquired at 25 °C in the 220–320 nm wavelength range with a 50 nm/min scanning rate. Each CD spectrum corresponds to an average of three scans, and the buffer baseline was subtracted from each spectrum. The DNA concentration was 10 µM and the Phen-DC_3 concentration ranged from 0 to 30 µM.

Electrospray ionization mass spectrometry (ESI-MS)

All ESI-MS experiments were performed in negative ion mode on an Agilent 6560 IMS-Q-TOF (Agilent Technologies, Santa Clara, CA, USA) and Thermo Orbitrap Exactive mass spectrometer with mild tuning conditions as described elsewhere.[2,3] The DNA and DNA-ligand complex solutions were incubated for 48 hours at 25 °C prior to injection. The injected DNA concentrations were 10-20 μM in 100 mM TMAA and 0.1-1 mM KCl (180 μL/h flow rate with a syringe pump).

Nuclear Magnetic Resonance Spectroscopy (NMR)

NMR experiments were performed on a Bruker AVANCE NEO 600, and 800 MHz spectrometer equipped with a QCI and TCI cryoprobe, respectively. All NMR experiments were performed in 95% H_2O+5% ^2H_2O (v/v) or 99.94% ^2H_2O (v/v) with DNA concentrations ranging between 0.1 and 0.5 mM. ^1H NMR experiments were performed with a spectral width of 20 ppm, 64 or 128 scans, 16 or 32 dummy scans, and a relaxation delay of 3 sec. 2D ^1H-^1H NOESY (τ_m = 100, 200 and 300 ms) and ^1H-^1H TOCSY (spinlock mixing time 40 and 60 ms) experiments were acquired with 2048 and 456 complex data points in *F2* and *F1* dimensions, respectively. Water suppression was achieved with the jump and return, 3-9-19 WATERGATE, and excitation sculpting block during the 1D and 2D experiments. For the residue-specifically ^{15}N- and ^{13}C-isotope labeled oligonucleotides, X-edited HSQC experiments were performed to assign the imino, aromatic and methyl resonances and confirmed by natural abundance ^1H–^{13}C HSQC acquired on the unlabeled DNA-ligand complex in 99.94% ^2D_2O.[4] ^1H NMR chemical shift were referenced with respect to the signal at δ2.60 ppm corresponding to DMSO-d_6. All NMR spectra were processed and analyzed with Topspin 4.07 (Bruker, Germany) and NMRFAM-SPARKY (Madison, USA) software.[5]

Structure calculations and restraints

The distance restraints for exchangeable and nonexchangeable protons were obtained from 2D NOESY (τ_m = 300 ms). The integral volumes of NOE cross-peaks corresponding to interproton distances were classified as strong (1.8−3.6 Å), medium (2.6−5.0 Å), and weak (3.5−6.5 Å) according to the averaged value obtained for thymine(s) methyl (Me)-H6 cross-peaks corresponding to 2.99 Å. 16 hydrogen-bond restrains (1.9–2.1 Å or 1.7–1.9 Å for acceptor–donor pairs N7-H21 or O6-H1, respectively) and 24 planarity restraints were used to constrain the formation of the quartets (G4-G10-G16-G22) and (G5-G9-G17-G21). For residues G3, G4, G9, G15, G16, and G21, the glycosidic bond torsion angle (χ) was restrained to *syn* conformation (60° ± 35°) based on the strong intra-residue H8-H1' NOE correlations, while for all other residues (guanines, adenines, and thymines) the χ angle was restrained to adopt *anti* conformation, i.e., 240° ± 70°.

The structure calculations were performed using Amber 20 software and the parmbsc1 force field, with parm χOL4 and parm ε/zOL1 modifications relying on the Born implicit solvent model and random starting velocities.[6–9] The partial charges for Phen-DC_3 were derived using the RESP ESP charge Derive Server (R.E.D) as described elsewhere.[10–12] Three rounds of restrained simulated annealing (SA), each 1000 ps long, were used. The force constants in the first SA were set to 5 kcal×mol^{-1}×Å^{-2} for NOE-based distance restraints, to 20 kcal×mol^{-1}×Å^{-2} for restraints corresponding to

hydrogen-bonds and planarity of guanine residues within individual G-quartets, 200 kcal×mol^{-1}×Å^{-2} for glycosidic torsion angles (χ) restraints and to 500 kcal×mol^{-1}×Å^{-2} for chirality. In the second and third rounds of SA calculations, the force constants for the NOE-based distance restraints were set to 20 kcal×mol^{-1}×Å^{-2}, while for other restraints, they were the same as in the first SA. According to the SA protocol, the force constants for the restraints were scaled from the initial value 0.1 to the final value 1.0 in the first 500 ps and held constant until the end of the calculation. Notably, the restraints for planarities of guanine residues within G-quartets were omitted after the first 500 ps of SA. SA protocol included heating over the first 100 ps from 300 to 1000 K, followed by 400 ps equilibration at 1000 K, cooling over 400 ps from 1000 to 0 K, and equilibration for 100 ps at 0 K.

The ‘model 1’ from the PDB entry ‘2JSM’ was used as the initial structure in the first SA calculation round to derive the structure exhibiting G-quadruplex topology in line with the experimental NMR-derived data for the complex.[13] The first SA calculation round relied on NOE-derived restraints corresponding to interproton interactions within DNA, excluding those for residues T1-G3, G11-G15, and G23. The lowest energy structure out of the total 100 calculated in the first SA was used as the starting structure for the second SA calculation round that relied on the use of NOE-derived restraints corresponding to interproton interactions within DNA, within the ligand, and between the DNA and ligand, excluding the ones for residues T1-G3, G11-G15, and G23. The lowest energy structure out of the total of 100 calculated in the second round of SA calculation was used as the starting structure of the third and final round of SA calculation. In the final SA calculation, all NMR-derived restraints were used along with three additional repulsive restraints (A2H2-T13Me, A2H2-T13 H2’, A2H2-T13 H2’’> 6.5 Å), which were applied to implement into the calculated model the lack of corresponding cross-peaks in NOESY NMR spectra.

Ten representative structures out of the total hundred calculated in the final SA round were selected based on the lowest energy criteria and subjected to energy minimization with a maximum of 10000 steps. The structures were analyzed and visualized with UCSF Chimera 1.15 software.[14]

In addition, unrestrained molecular dynamics was performed to calculate 10 structures according to 50 ns long protocol, in which the temperature was raised from 0 to 298 K during the first 1 ns and afterwards held constant at 298 K. The lowest energy model from the restrained SA calculations was used as the starting structure for the unrestrained molecular dynamics calculations.

Table S1. Sequences of 23TAG analogs

DNA name	#nt	Abbr.	Sequence*
23TAG_UN	23	23TAG	TA GGG TTA GGG TTA GGG TTA GGG
23TAG_G3	23	G3	TA **G**GG TTA GGG TTA GGG TTA GGG
23TAG_G4	23	G4	TA G**G**G TTA GGG TTA GGG TTA GGG
23TAG_G5	23	G5	TA GG**G** TTA GGG TTA GGG TTA GGG
23TAG_G9	23	G9	TA GGG TTA **G**GG TTA GGG TTA GGG
23TAG_G10	23	G10	TA GGG TTA G**G**G TTA GGG TTA GGG
23TAG_G11	23	G11	TA GGG TTA GG**G** TTA GGG TTA GGG
23TAG_G15	23	G15	TA GGG TTA GGG TTA **G** GG TTA GGG
23TAG_G16	23	G16	TA GGG TTA GGG TTA G**G**G TTA GGG
23TAG_G17	23	G17	TA GGG TTA GGG TTA GG**G** TTA GGG
23TAG_G21	23	G21	TA GGG TTA GGG TTA GGG TTA **G**GG
23TAG_G22	23	G22	TA GGG TTA GGG TTA GGG TTA G**G**G
23TAG_G23	23	G23	TA GGG TTA GGG TTA GGG TTA GG**G**
23TAG_T1	23	T1	**T**A GGG TTA GGG TTA GGG TTA GGG
23TAG_T6	23	T6	TA GGG **T**TA GGG TTA GGG TTA GGG
23TAG_T7	23	T7	TA GGG T**T**A GGG TTA GGG TTA GGG
23TAG_T12	23	T12	TA GGG TTA GGG **T**TA GGG TTA GGG
23TAG_T13	23	T13	TA GGG TTA GGG T**T**A GGG TTA GGG
23TAG_T18	23	T18	TA GGG TTA GGG TTA GGG **T**TA GGG
23TAG_T19	23	T19	TA GGG TTA GGG TTA GGG T**T**A GGG
23TAG_A2	23	A2	T**A** GGG TTA GGG TTA GGG TTA GGG
23TAG_A8	23	A8	TA GGG TT**A** GGG TTA GGG TTA GGG
23TAG_A14	23	A14	TA GGG TTA GGG TT**A** GGG TTA GGG
23TAG_A20	23	A20	TA GGG TTA GGG TTA GGG TT**A** GGG

* The selective ^{15}N and ^{13}C labeling is marked in bold letters.

Table S2. ^{1}H NMR chemical shifts of 23TAG in 23TAG+Phen-DC$_3$ complex*

Residue	H1/H2/H3	Me	H6/H8	H1'	H2', H2''	H3'	H4'	H5', H5''
T1		0.86	6.66	5.17	0.95, 1.46	3.96	3.31	2.95
A2	7.41		7.76	5.71				
G3			6.76	6.03	3.02, 2.85	5.63	4.20	
G4	11.21		6.65	5.68	3.18, 2.67	4.92	4.35	
G5	11.24		7.37	5.64	2.52, 2.43	5.08	4.25	4.15
T6		1.92	7.80	6.2	2.24, 2.39	4.82	4.33	4.07, 4.22
T7		1.52	7.11	5.72	1.07, 1.92	4.60	4.05	3.87, 3.81
A8	7.75		7.96	5.96	2.71, 2.60	4.90	4.17	3.89, 3.70
G9	11.27		7.19	5.84	3.31, 2.78	4.89	4.26	
G10	11.36		7.67	5.78	2.53, 2.58	5.09	4.28	4.15
G11			8.07	5.88	2.81, 2.58	4.98	4.51	4.28
T12		1.93	7.76	6.33	2.37, 2.55	4.89	4.49	4.14, 4.21
T13		1.53	7.54	6.14	1.84, 2.19	4.50	4.16	4.04
A14	7.55		7.10	5.71	1.80, 2.50	4.60	4.05	3.85, 3.81
G15	10.16		7.51	6.11	2.82, 2.92	5.46	4.20	4.08
G16	10.54		7.13	5.82	2.87, 2.58	4.81	4.44	
G17	11.21		7.36	5.71	2.46, 2.49	5.08	4.27	4.16
T18		1.93	7.80	6.21	2.25, 2.39	4.82	4.33	4.07, 4.22
T19		1.52	7.11	5.73	1.09, 1.93	4.61	4.05	3.86, 3.80
A20	7.78		7.99	6.02	2.74, 2.62	4.91	4.19	3.91, 3.71
G21	11.22		7.03	5.81	3.30, 2.77	4.91	4.29	4.16
G22	11.17		8.06	5.39	2.67, 2.66	5.08	4.27	4.16
G23	10.02		7.51	5.60	2.67, 2.39	4.51	4.21	4.40, 4.12

* Spectra were acquired in 95% H_2O/5% $^{2}H_2O$ at 25 °C, 70 mM KCl, 20 mM potassium-phosphate buffer (pH 7.0). Assignments of H5/H5” are not stereospecific.

Table S3. ^{1}H NMR chemical shifts of Phen-DC_3 in 23TAG+Phen-DC_3 complex*

Phen-DC_3 atom(s)	Chemical shift (ppm)
HA/HA'	12.07
HB	9.05
HB'	8.92
HC	10.06
HC'	10.28
HD	7.86
HD'	7.60
HE	7.43
HE'	7.39
HF	7.11
HF'	6.92
HG	7.50
HG'	7.10
HI	4.70
HI'	4.51
HH	7.25
HH'	7.23
HJ	8.50
HJ'	8.35
HK	8.21
HK'	8.11

* Spectra were acquired in 95% H_2O/5% $^{2}H_2O$ at 25 °C, 70 mM KCl, 20 mM potassium-phosphate buffer (pH 7.0).

Table S4. Intermolecular NOE restraints between 23TAG-G4 and Phen-DC$_3$ in the 1:1 23TAG-G4+Phen-DC$_3$ complex*

Phen-DC$_3$		HA	HA'	HB	HB'	HC	HC'	HD	HD'	HE	HE'	HF	HF'	HG	HG'	HI	HI'	HH	HH'	HJ	HJ'	HK	HK'
G3	H8																		m		m		w
	H1'																		m		w		
	H2'						w												m		m		
	H2"						w												s		m		
	H3'						w												m				
	H4'																		w				
G4	H8																		m		m		w
	H1		w	w	w		w																
	H1'																				w		
	H4'						w												m				
G10	H8						w						w		m		m						
	H1			w	w			w	m		w												
	H1'										w		m										
	H2'												w										
	H2"												m										
G11	H8												m		m		m						
	H1'																						
	H2'														w								
	H2"														w								
	H5'												w										
G15	H1	w		w																			
	H2'					w						w		m									
	H2"											w		m									
	H3'															w							
G16	H1	w		w		w																	
	H1'													w									
	H3'													w									
G22	H8					m												w					
	H1	w																					
	H1'																	m		m		w	
	H2"					w												m		m			
	H3'																	w					
G23	H1'																			w			
	H3'																			w			
	H4'																			m			
	H5'																	m		m			
	H5"																	w		m			

* NOE cross-peak intensities are classified as strong (s), medium (m), and weak (w).

Table S5. NMR restraints and structural statistics for the 23TAG+Phen-DC_3 complex structure

Distance and torsion angle restraints		
NOE-derived distance restraints	non – exchangeable	exchangeable
Intra-nucleotide DNA-DNA NOEs	250	0
Sequential DNA-DNA (|i – j| = 1)	116	7
Long-range DNA-DNA (|i – j| > 1)	32	12
DNA-ligand	58	15
ligand-ligand	4	0
repulsive DNA-DNA	3	0
Torsion angle restraints	23	
Hydrogen-bond restraints[a]	16	
Planarity restrains[a]	24	
Structural statistics (mean from 10 representative structures)		
NOE violations >0.2Å	0	
Torsion angle restraint violation >0.2°	0	
[b]Pairwise atom R.M.S.D. (Å)		
Overall		0.675 (0.561)
Without 5' TA overhang		0.651 (0.545)
Without 5' TA overhang and residues T12, T13, A14		0.597 (0.502)
Only guanine residues and Phen-DC_3		0.638 (0.574)

[a] H-bonding and planarity restrain used for the G4-G10-G16-G22 and G5-G9-G17-G21 quartets.
[b] The numbers in the brackets correspond to the R.M.S.D. value when considering heavy atoms (C, O, N, P) only.

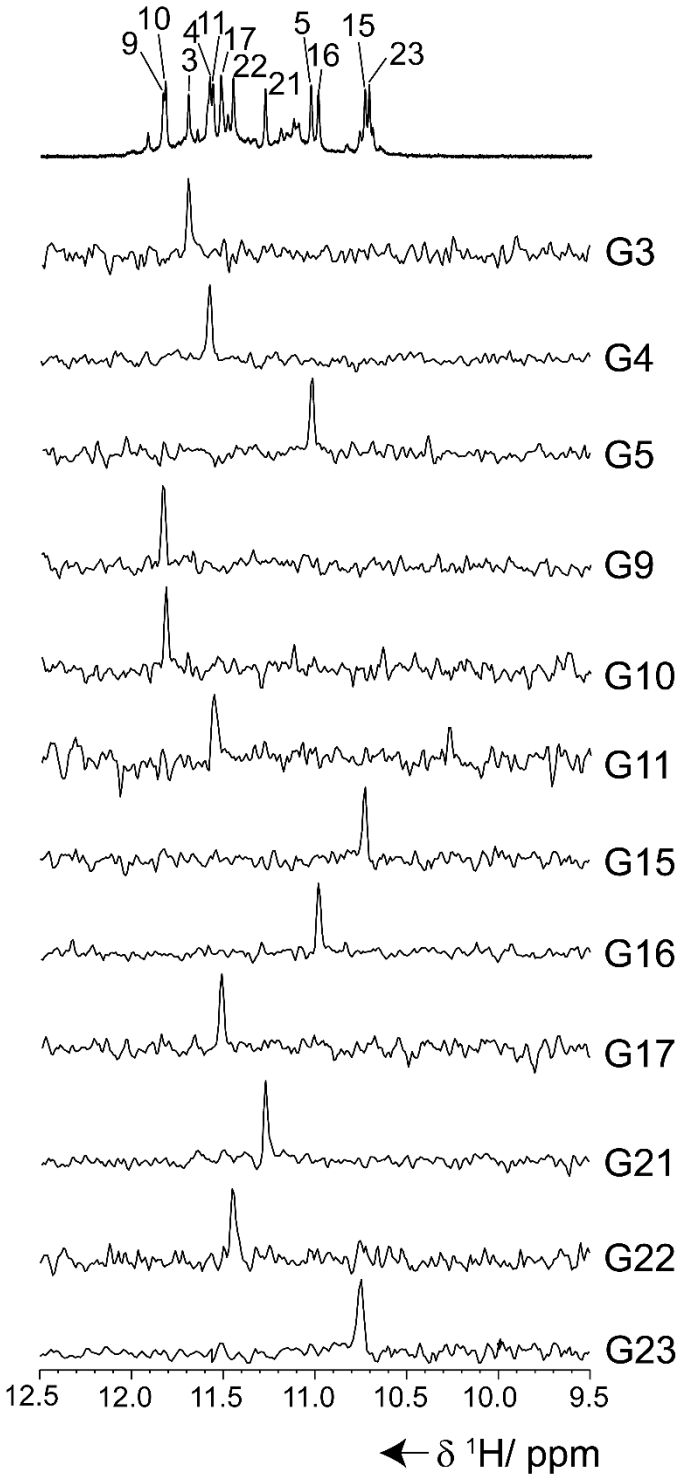

Figure S1. Assignment of guanine imino proton (H1) ^{1}H NMR resonances of 23TAG. 1D ^{15}N-filtered HSQC spectra of samples containing residue specific partially (4-8%) ^{15}N-labelled 23TAG-G4. All spectra were recorded on a 600 MHz NMR spectrometer in 95% H_2O/5% $^{2}H_2O$ at 25 °C, 70 mM KCl, 20 mM potassium phosphate buffer (pH 7.0) and 200 µM oligonucleotide concentration per strand.

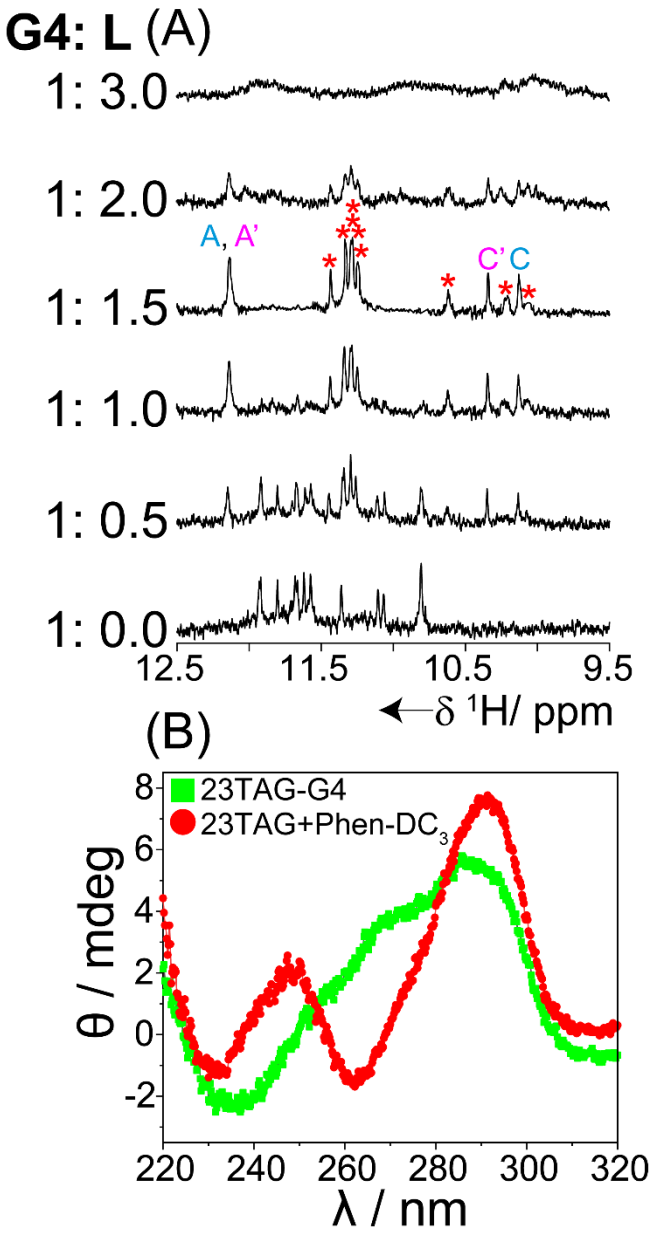

Figure S2. Interaction of 23TAG with Phen-DC$_3$ analyzed by ^{1}H NMR and CD in 100 mM TMAA and 1 mM KCl. (A) Imino region of the ^{1}H NMR spectra of 23TAG-G4 upon titration with Phen-DC$_3$ to up to 3 mole equivalents. The imino proton signals for 23TAG+Phen-DC$_3$ complex are marked with red stars. ^{1}H NMR spectra were recorded on a 600 MHz NMR spectrometer in 95% H_2O/5% ^2H_2O at 25 °C, 1 mM KCl, 100 mM TMAA buffer (pH 7.0) and 100 µM oligonucleotide concentration per strand. (B) CD spectra of 23TAG-G4 alone (green) and in the presence of 1.5 molar equivalent of Phen-DC$_3$ (red). CD spectra were recorded at 25 °C, 1 mM KCl, 100 mM TMAA buffer (pH 7.0) and 10 µM oligonucleotide concentration per strand.

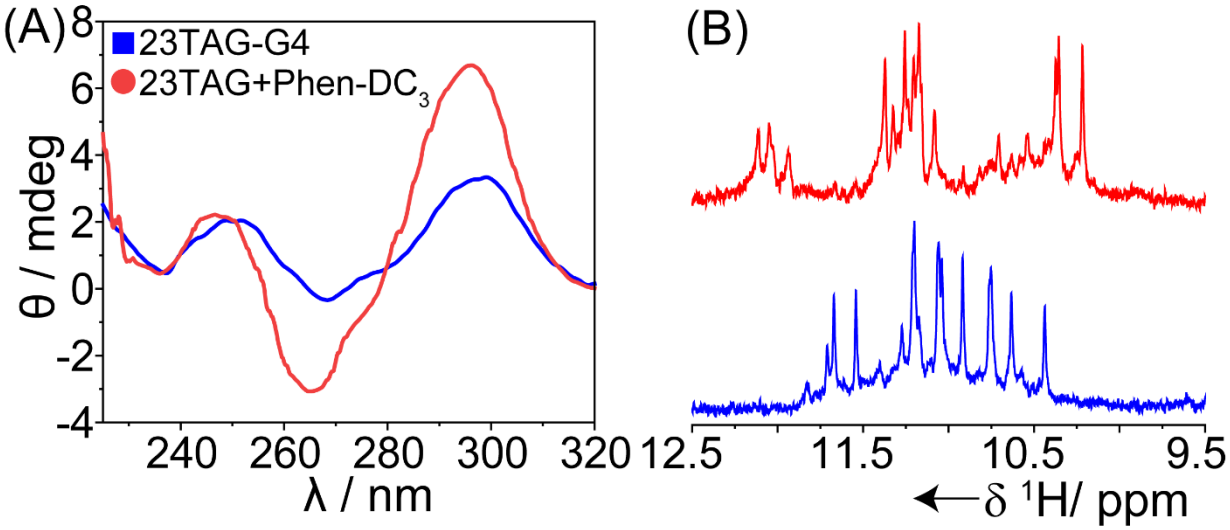

Figure S3. Phen-DC$_3$ induced conformational change of 23TAG in Na$^+$ ion environment. (A) CD spectra of 10 µM 23TAG-G4 alone (blue) and in the presence of 1.5 molar equivalent of Phen-DC$_3$ (red) at 25 °C in 150 mM Na$^+$ and 10 mM Tris–HCl (pH 7.5). (B) Imino region of the ^{1}H NMR spectra of 100 µM 23TAG-G4 alone (blue) and in the presence of Phen-DC$_3$ at 1.5 molar equivalent (red). ^{1}H NMR spectra were recorded on a 600 MHz NMR spectrometer in 95% H_2O/5% ^2H_2O at 25 °C, 150 mM NaCl, 10 mM Tris–HCl buffer (pH 7.5).

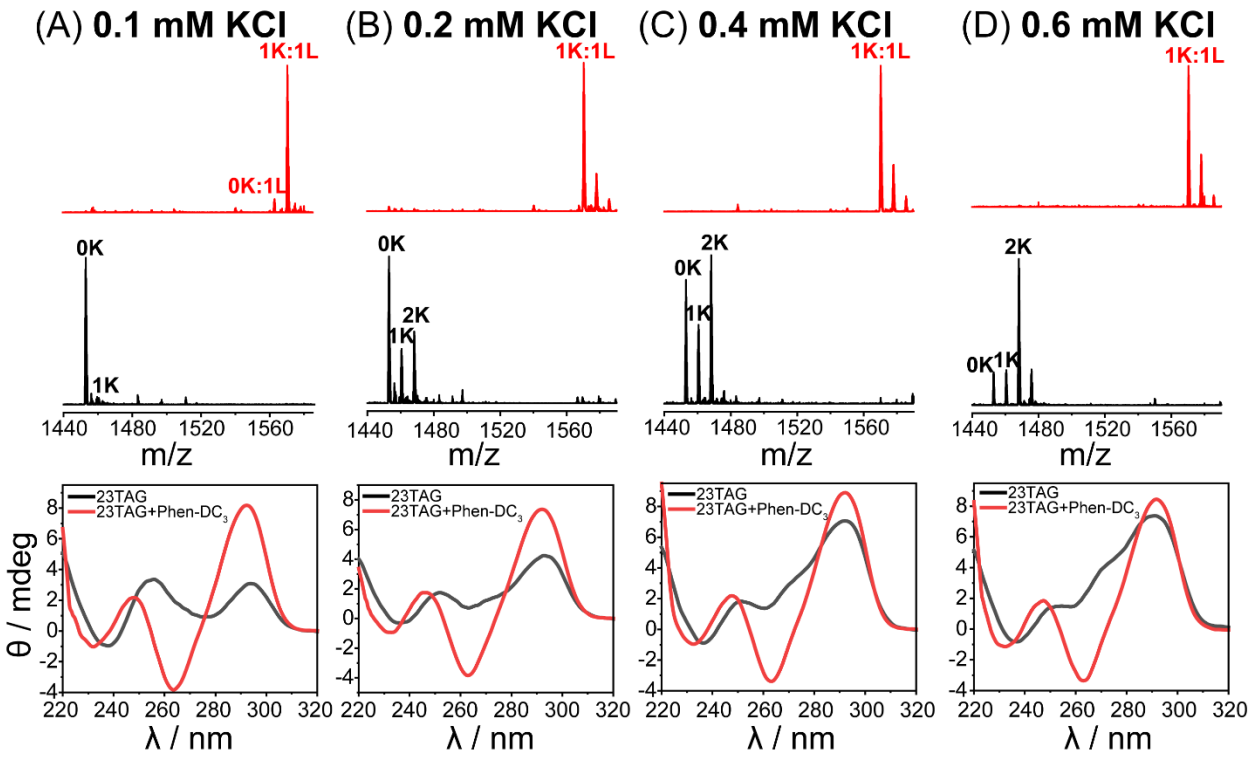

Figure S4. Effect of Phen-DC$_3$ on the 23TAG conformation at different concentrations of KCl analyzed by ESI-MS and CD. (Top panel) ESI-MS spectra of 23TAG (black) and in presence of Phen-DC$_3$ (red) at 1:1 molar equivalent. 0K, 1K and 2K denote 0, one potassium and two potassium cations bound 23TAG, and 23TAG-Phen-DC$_3$ complex, respectively. (Bottom panel) CD spectra of 23TAG (black) and in presence of Phen-DC$_3$ (red) at 1:1 molar equivalent. The ESI-MS and CD spectra were recorded in 100 mM TMAA (pH 7.0), at 25 °C, 10 μM oligonucleotide concentration per strand and (A) 0.1 mM KCl (B) 0.2 mM KCl (C) 0.4 mM KCl (D) 0.6 mM KCl.

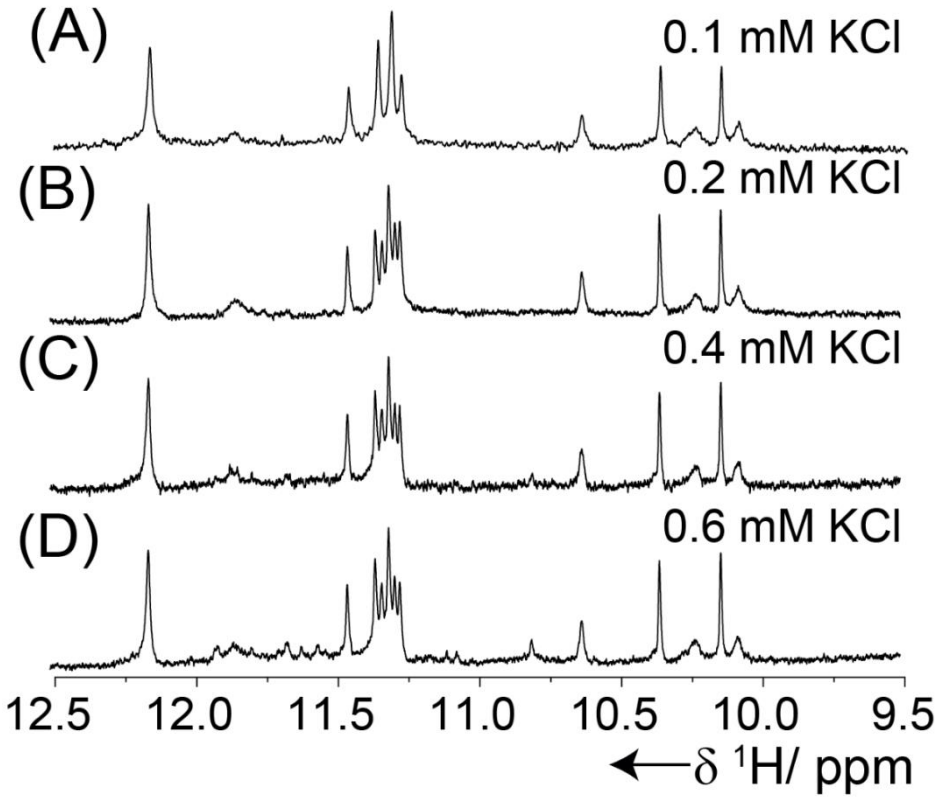

Figure S5. Effect of Phen-DC$_3$ on 23TAG conformation at different concentrations of KCl monitored by ^{1}H NMR. Imino region of the ^{1}H NMR spectra of 100 µM 23TAG in the presence of Phen-DC3 at a 1:1 molar equivalent at (A) 0.1 mM KCl (B) 0.2 mM KCl (C) 0.4 mM KCl (D) 0.6 mM KCl. The ^{1}H NMR spectra were recorded on a 600 MHz NMR spectrometer in 95% H_2O/5% ^2H_2O at 25 °C and 100 mM TMAA (pH 7.0).

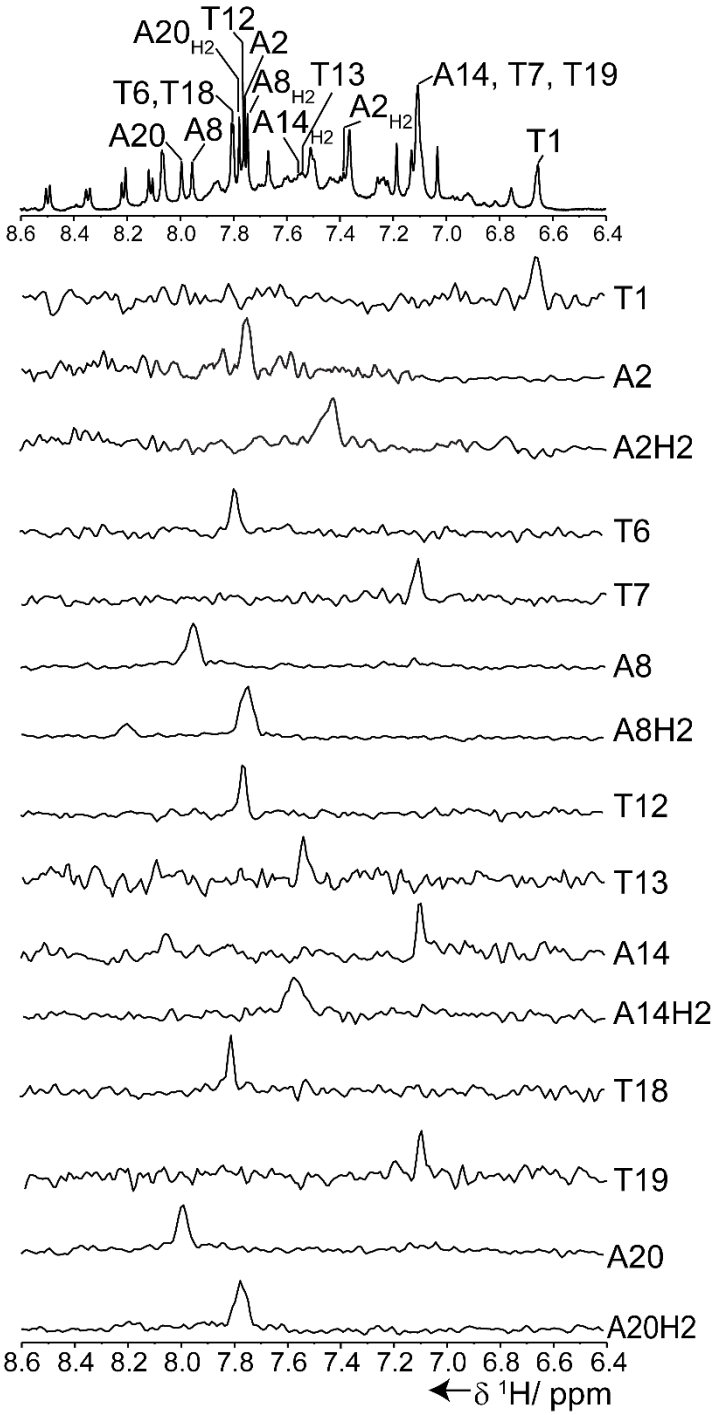

Figure S6. Assignment of aromatic ^{1}H NMR resonances of adenine (H8, H2) and thymine (H6) of the 23TAG+Phen-DC$_3$ complex. 1D slices from ^{13}C-filtered HSQC spectra of samples containing residue specific partially (4-8%) ^{13}C-isotopically labelled 23TAG-G4+Phen-DC$_3$ complex. All spectra were recorded on a 600 MHz NMR spectrometer in 95% H_2O/5% $^{2}H_2O$, at 25 °C, 70 mM KCl, 20 mM potassium phosphate buffer (pH 7.0). The concentrations of 23TAG-G4 and Phen-DC$_3$ were 200 and 300 µM, respectively.

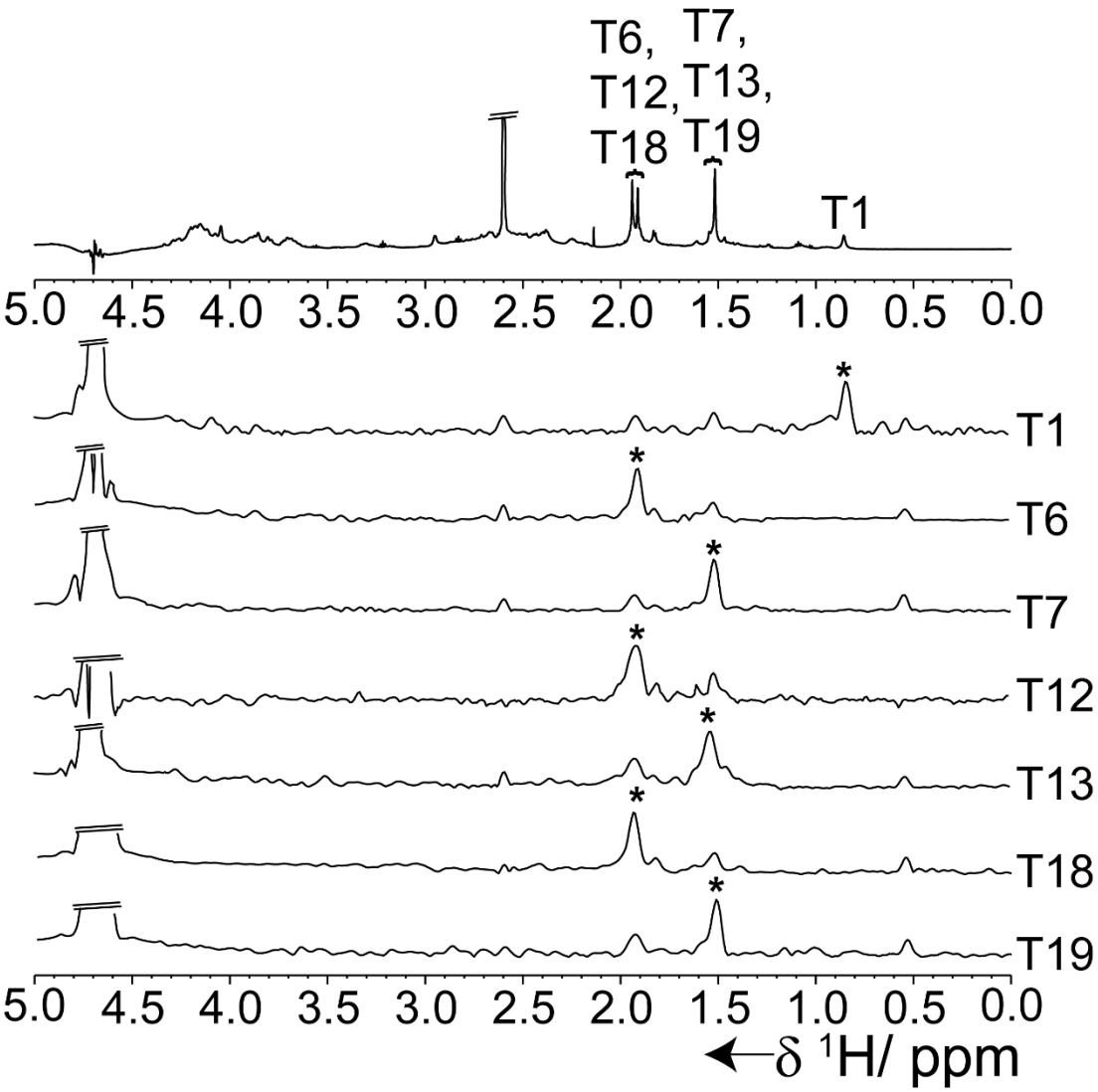

Figure S7. Assignment of thymine methyl ^{1}H NMR resonances of 23TAG+Phen-DC$_3$ complex. 1D slices from ^{13}C-filtered HSQC spectra of samples containing residue specific partially (4-8%) ^{13}C-isotopically labelled 23TAG-G4+Phen-DC$_3$ complex. All spectra were recorded on a 600 MHz NMR spectrometer in 95% H_2O/5% $^{2}H_2O$, at 25 °C in 70 mM KCl, 20 mM potassium phosphate buffer (pH 7.0). The concentrations of 23TAG-G4 and Phen-DC$_3$ were 200 and 300 µM, respectively.

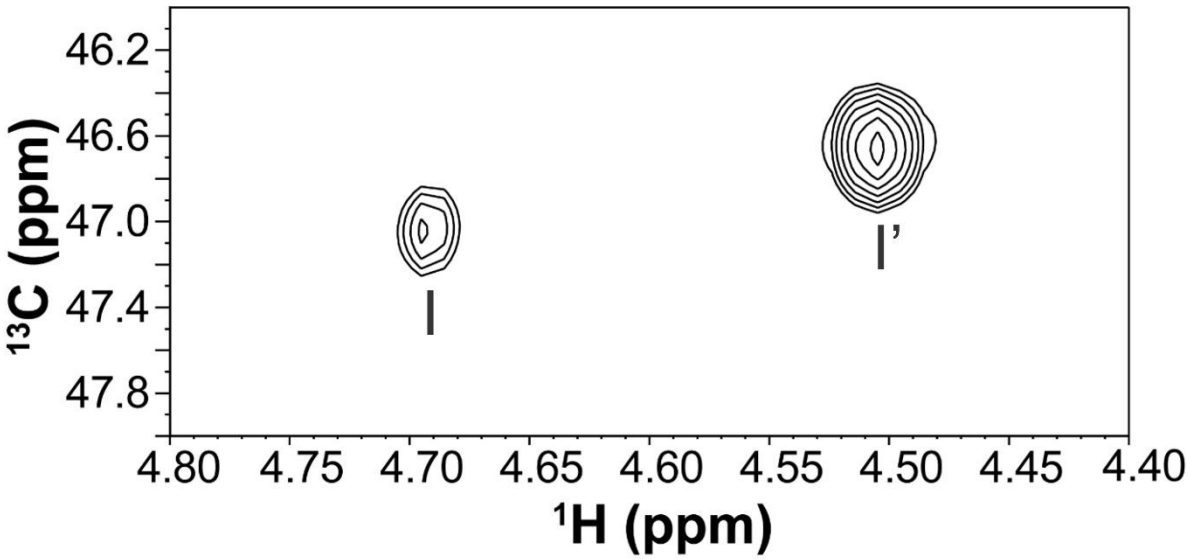

Figure S8. Assignment of Phen-DC$_3$ N-methyl (I and I') ^{1}H NMR resonances of the 23TAG+Phen-DC$_3$ complex. ^{1}H-^{13}C HSQC spectrum of the 23TAG+Phen-DC$_3$ (^{13}C-Methyl labelled) complex showing the signals of the ^{13}C-labeled N-methyl groups of Phen-DC$_3$. All spectra were recorded on a 600 MHz NMR spectrometer in 95% H_2O/5% $^{2}H_2O$, at 25 °C, 20 mM KCl, 70 mM potassium phosphate buffer (pH 7.0). The concentrations of 23TAG-G4 and Phen-DC$_3$ were 200 and 300 µM, respectively.

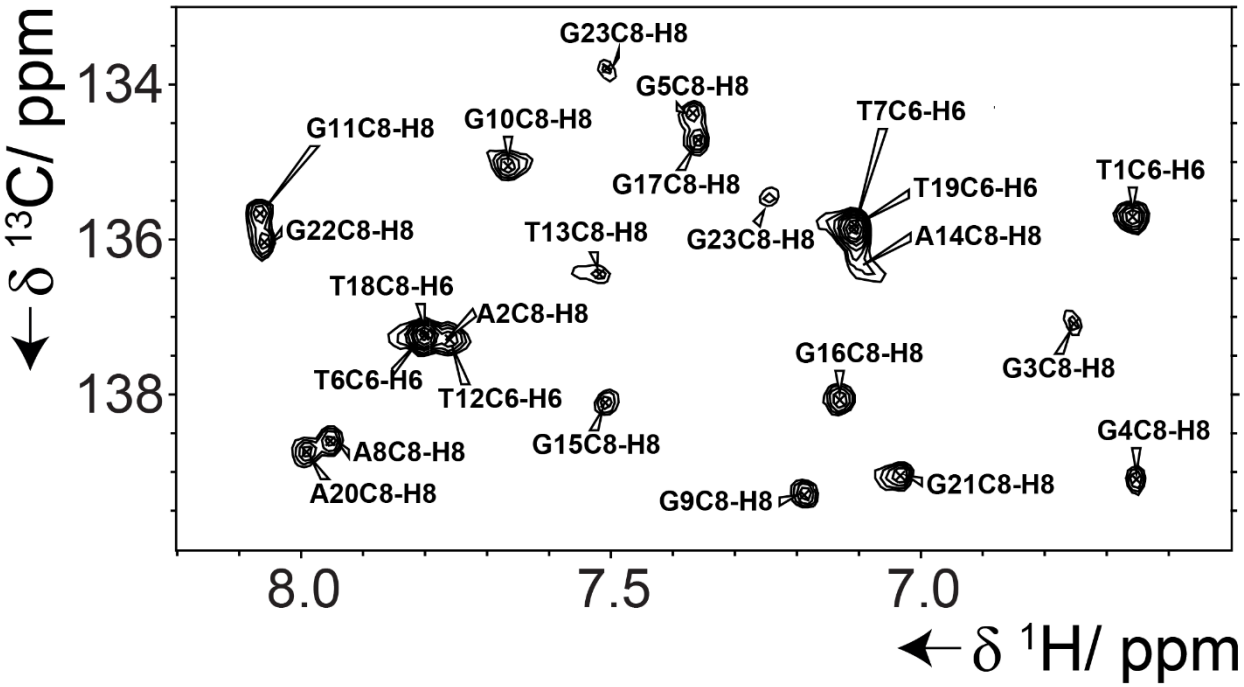

Figure S9. Assignment of adenine, guanine and thymine aromatic ^{1}H and ^{13}C NMR resonances in the 23TAG+Phen-DC$_3$ complex. Spectral region of the 2D natural abundance ^{1}H–^{13}C HSQC spectrum of 23TAG+Phen-DC$_3$ complex showing the H6−C6/H8−C8 cross-peaks for all nucleotides. All spectra were recorded on a 600 MHz NMR spectrometer in 95% H_2O/5% $^{2}H_2O$, at 25 °C, 70 mM KCl, 20 mM potassium phosphate buffer (pH 7.0). The concentrations of 23TAG-G4 and Phen-DC$_3$ were 500 and 750 µM, respectively.

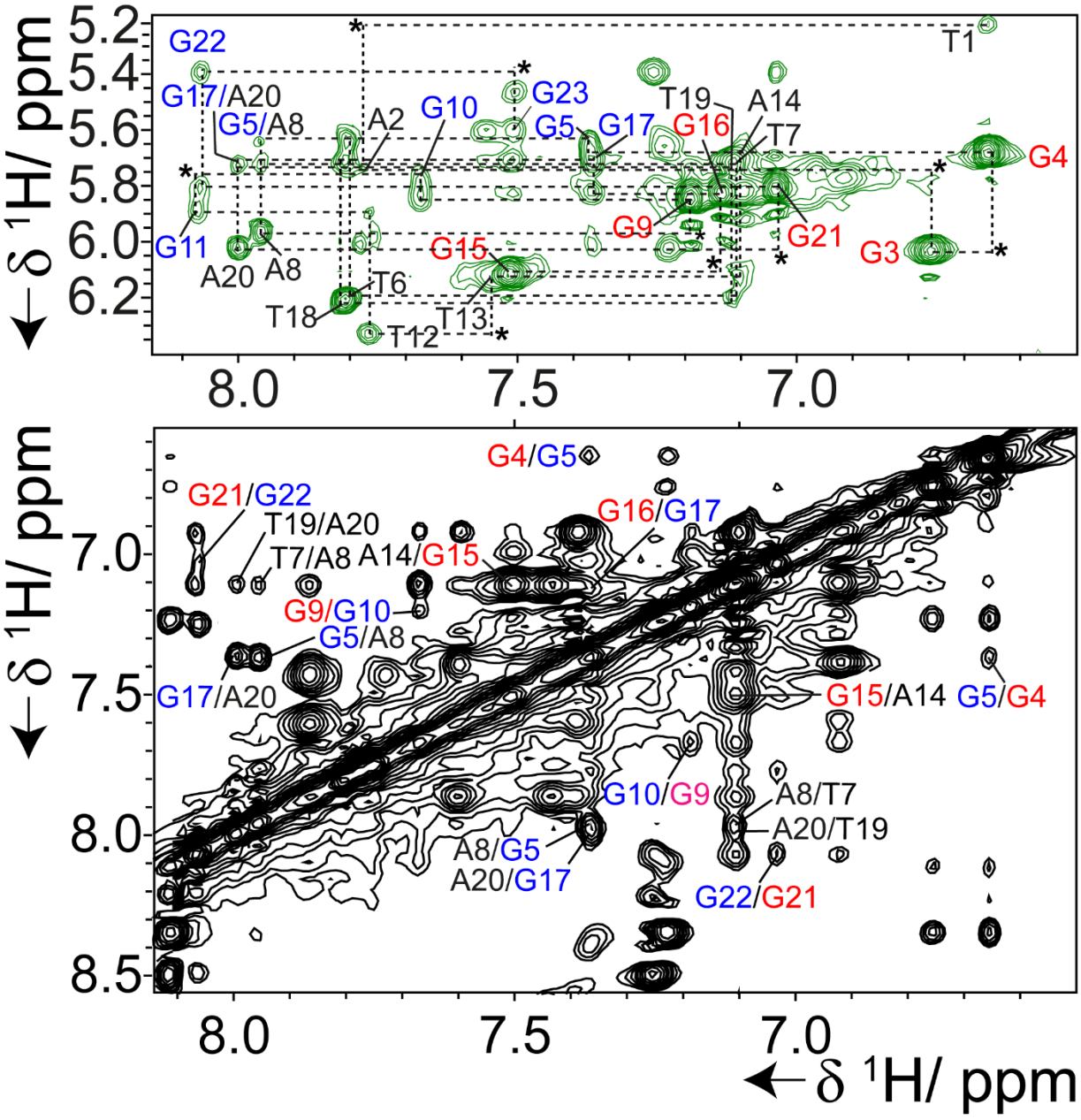

Figure S10. Analysis of the folding topology of 23TAG+Phen-DC$_3$ complex by 2D ^{1}H-^{1}H NOESY. (Top panel) Intra-residual, sequential (i to i+1), and long range H1′-H6/H8 correlations traced by dashed black lines in the anomeric-aromatic region of the NOESY spectrum (τ_m = 100 ms). The absence of sequential correlation is marked by '*'. (Bottom panel) Sequential and long range H6–H8/H8-H8 cross-peaks are marked in the aromatic region of the NOESY spectrum (τ_m = 300 ms). Guanines exhibiting *syn* and *anti* glycosidic bond angle conformations are labeled with red and blue color, respectively. All spectra were recorded on a 600 MHz NMR spectrometer in 95% H_2O/5% ^2H_2O, at 25 °C, 70 mM KCl, 20 mM potassium phosphate buffer (pH 7.0). The concentrations of 23TAG-G4 and Phen-DC$_3$ were 500 and 750 µM, respectively.

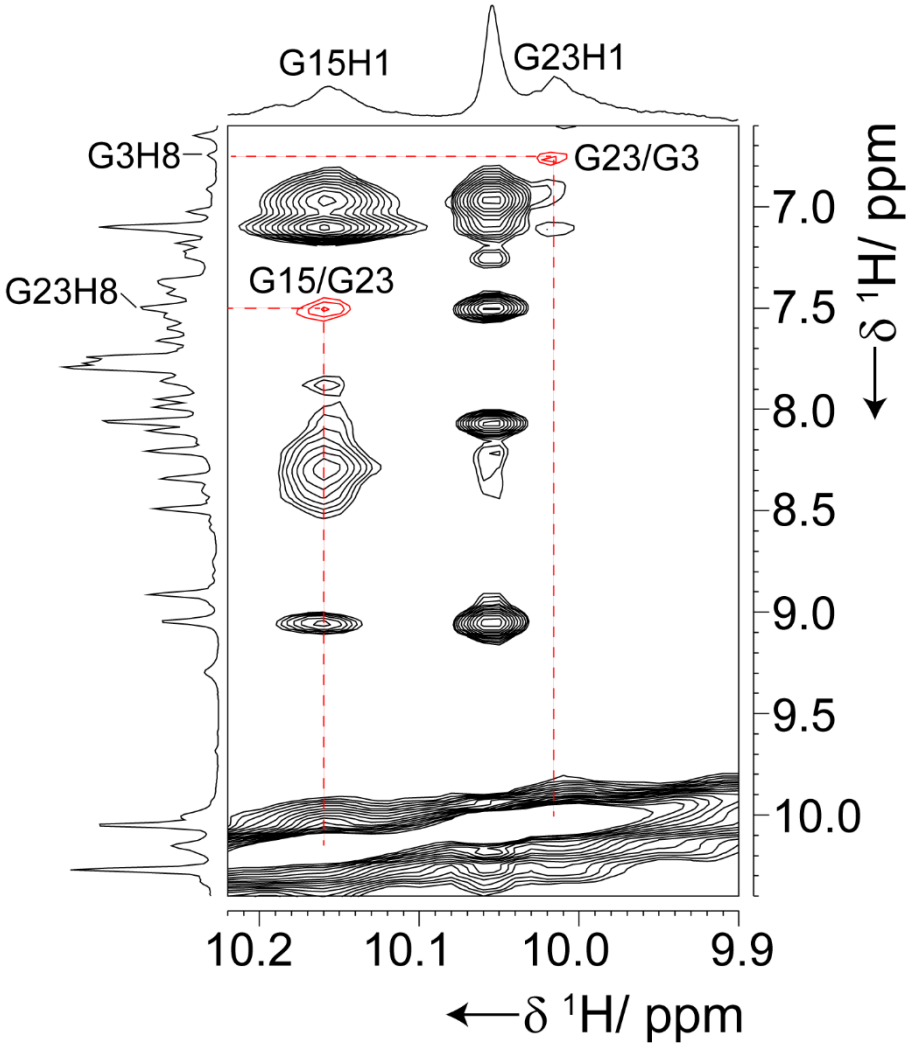

Figure S11. Imino-aromatic NOEs in the 23TAG+Phen-DC$_3$ complex. The region of 2D ^{1}H-^{1}H JR NOESY spectrum (τ_m = 300 ms) showing G15H1-G23H8 and G23H1-G3H8 NOE cross-peaks (red) in G3→G11→G15→G23 'pseudo-quartet'. The spectrum was recorded on an 800 MHz NMR spectrometer in 95% H_2O/5% ^2H_2O, at 25 °C 70 mM KCl, 20 mM potassium phosphate buffer (pH 7.0). The concentrations of 23TAG-G4 and Phen-DC$_3$ were 500 and 750 µM, respectively.

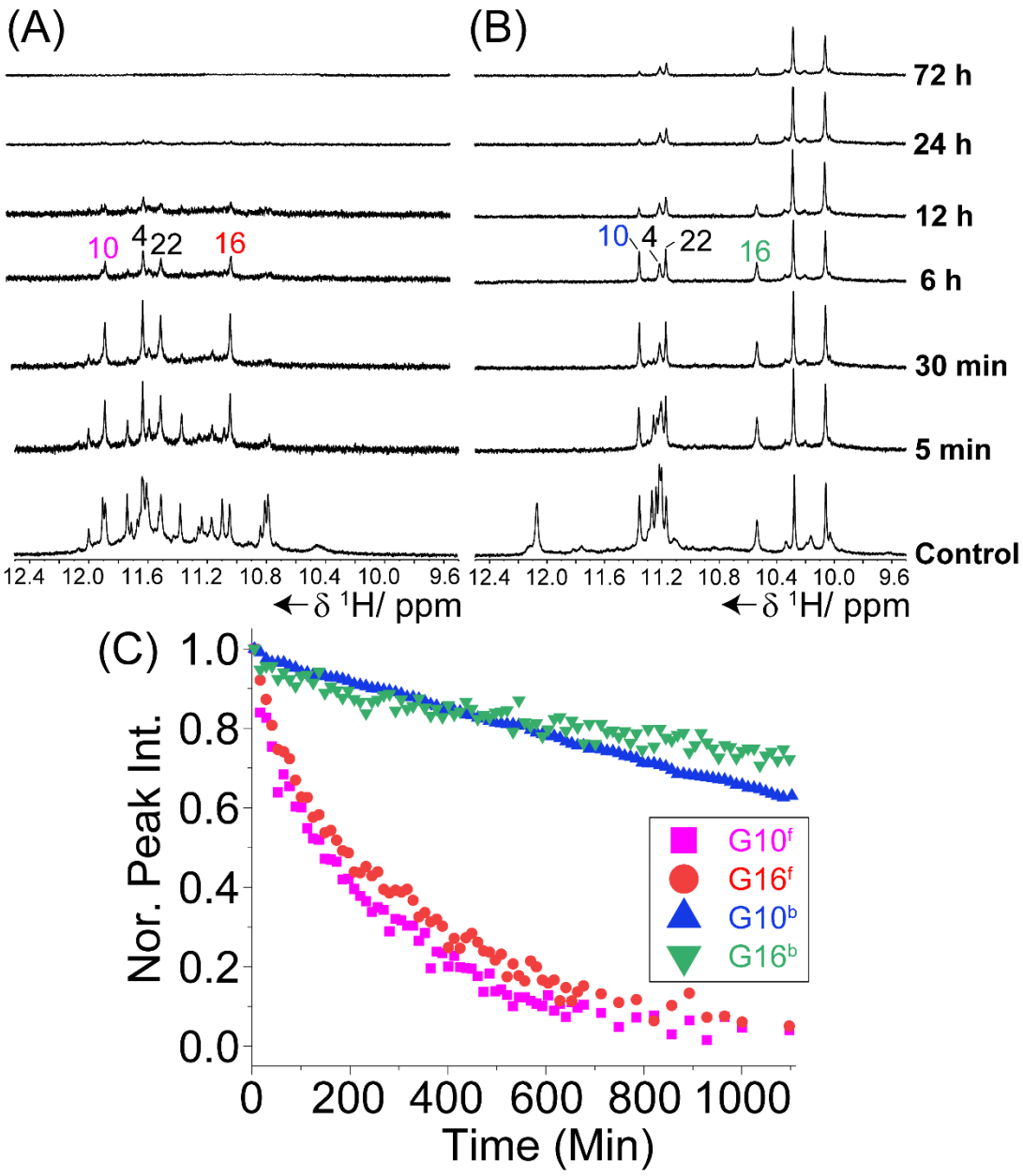

Figure S12. Analysis of imino proton exchange with the bulk solvent in 23TAG and 23TAG+Phen-DC$_3$ complex by HDX NMR. (A) Time dependent changes in imino proton (H1) intensities of the ^{1}H NMR spectra of 23TAG-G4 upon addition of ^2H_2O to the lyophilized sample. (B) Time dependent changes in imino proton (H1) intensities of 23TAG+Phen-DC$_3$ upon addition of ^2H_2O to lyophilized sample. The most protected imino protons (H1) after 6 hours are marked in the figure. (C) Time evolution of the G10 and G16 imino proton intensities of the 23TAG-G4 (subscript 'f') and 23TAG+Phen-DC$_3$ complex (subscript 'b'). All spectra were recorded on a 600 MHz NMR spectrometer at 25 °C by dissolving lyophilized sample containing 70 mM KCl, 20 mM potassium phosphate buffer (pH 7.0) in 99.94 % ^2H_2O. The concentrations of 23TAG-G4 and Phen-DC$_3$ were 500 and 750 µM, respectively.

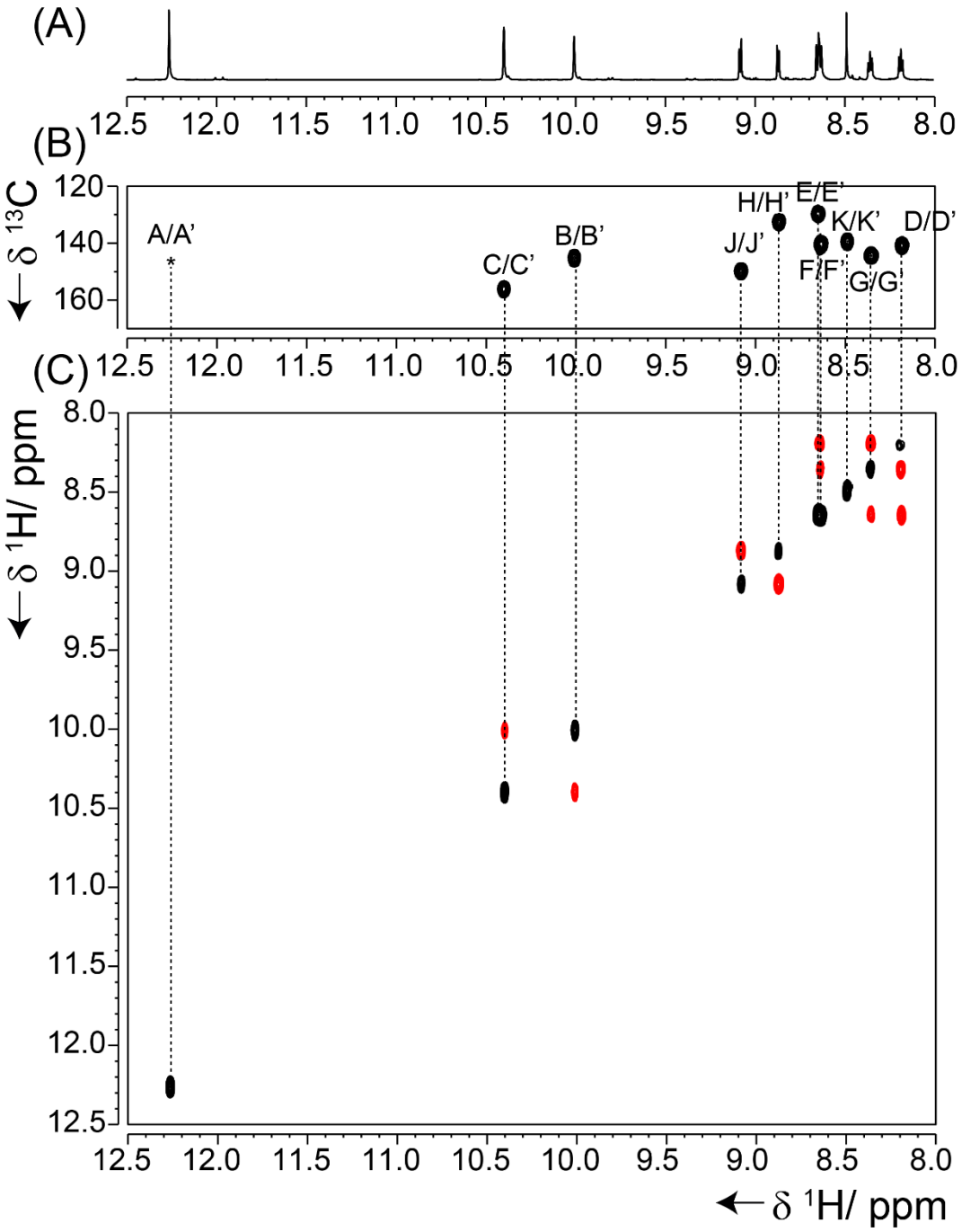

Figure S13. Assignment of Phen-DC$_3$ ^{1}H and ^{13}C NMR resonances in its free form (in DMSO-d$_6$). (A) 1D ^{1}H NMR and (B) natural abundance ^{1}H-^{13}C HSQC spectrum of Phen-DC$_3$. (C) TOCSY spectrum (mixing time 80 ms) of Phen-DC$_3$ showing the assignment and correlations between aromatic protons. The diagonal and off diagonal peaks are marked by black and red color, respectively. All spectra were recorded at 600 MHz NMR spectrometer in 99.96% DMSO-d$_6$, at 25 °C and 500 µM Phen-DC$_3$.

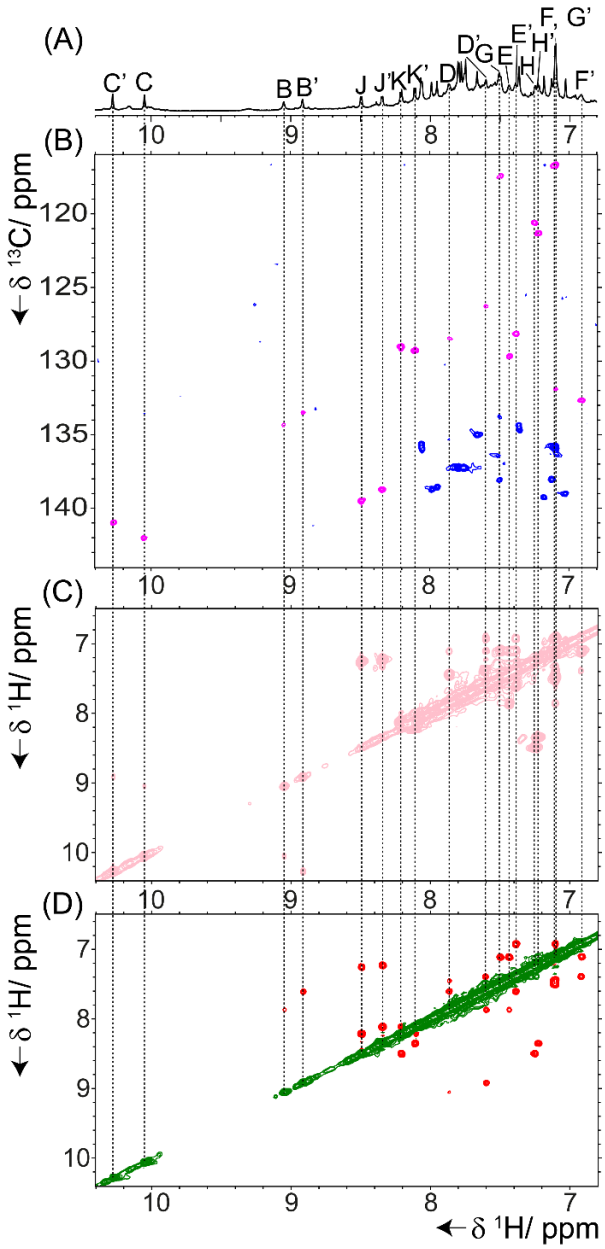

Figure S14. Assignment of Phen-DC$_3$ ^{1}H and ^{13}C NMR resonances in the 23TAG+Phen-DC$_3$ complex. (A) Aromatic region of 1D ^{1}H NMR of 23TAG+Phen-DC$_3$ complex. (B) Natural abundance ^{1}H-^{13}C HSQC of the 23TAG+Phen-DC$_3$ complex with Phen-DC$_3$ aromatic C-H peaks marked by magenta color. (C) ^{1}H-^{1}H TOCSY spectrum ((τ_m = 50 ms) of the 23TAG+Phen-DC$_3$ complex showing the through bond correlations between aromatic protons of Phen-DC$_3$. (D) ^{1}H-^{1}H ROESY spectrum (τ_m = 100 ms) of the 23TAG+Phen-DC$_3$ complex showing the correlations between aromatic protons of Phen-DC$_3$. The diagonal and off-diagonal peaks are marked by green and red color, respectively. All spectra were recorded on a 600 MHz NMR spectrometer in 99.94% ^2H_2O, at 25 °C, 70 mM KCl, 20 mM potassium phosphate buffer. The concentrations of 23TAG-G4 and Phen-DC$_3$ were 500 and 750 µM, respectively.

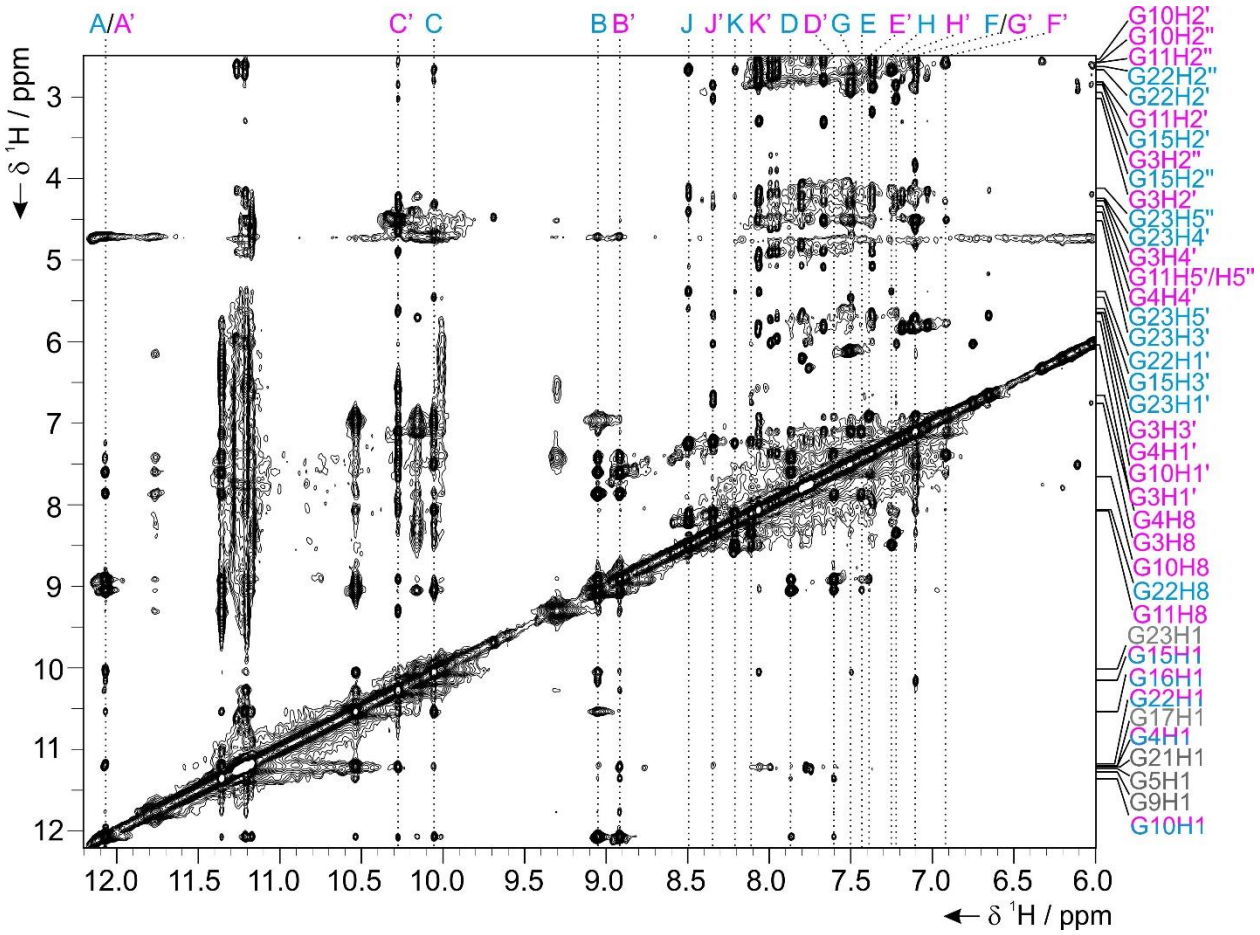

Figure S15. Inter-molecular interactions in the 23TAG+Phen-DC$_3$ complex. The region of 2D ^{1}H-^{1}H NOESY spectrum (τ_m = 300 ms) showing all inter-molecular NOE cross-peaks. The spectrum was recorded on a 600 MHz NMR spectrometer in 95% H_2O/5% ^2H_2O, at 25 °C 70 mM KCl, 20 mM potassium phosphate buffer (pH 7.0). The concentrations of 23TAG and Phen-DC$_3$ were 500 and 750 µM, respectively.

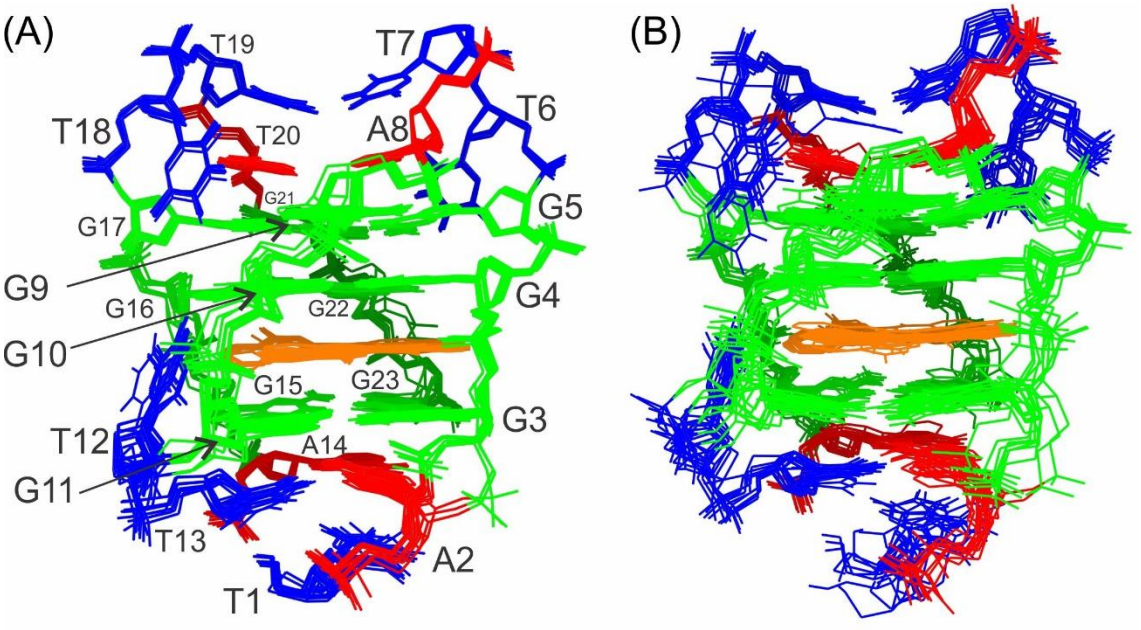

Figure S16. Comparison of the structures calculated with the use of restrained and unrestrained molecular dynamics. (A) Ten lowest energy structures of 23TAG+Phen-DC_3 complex obtained by 1 ns MD (SA) relying on NOE-based distance restraints, glycosidic torsion angles restraints as well as hydrogen-bonds and planarity restraints for the guanine residues within G5-G9-G17-G21 and G4-G10-G16-G22 quartets. (B) Ten structures obtained by unrestrained 50 ns MD calculations.

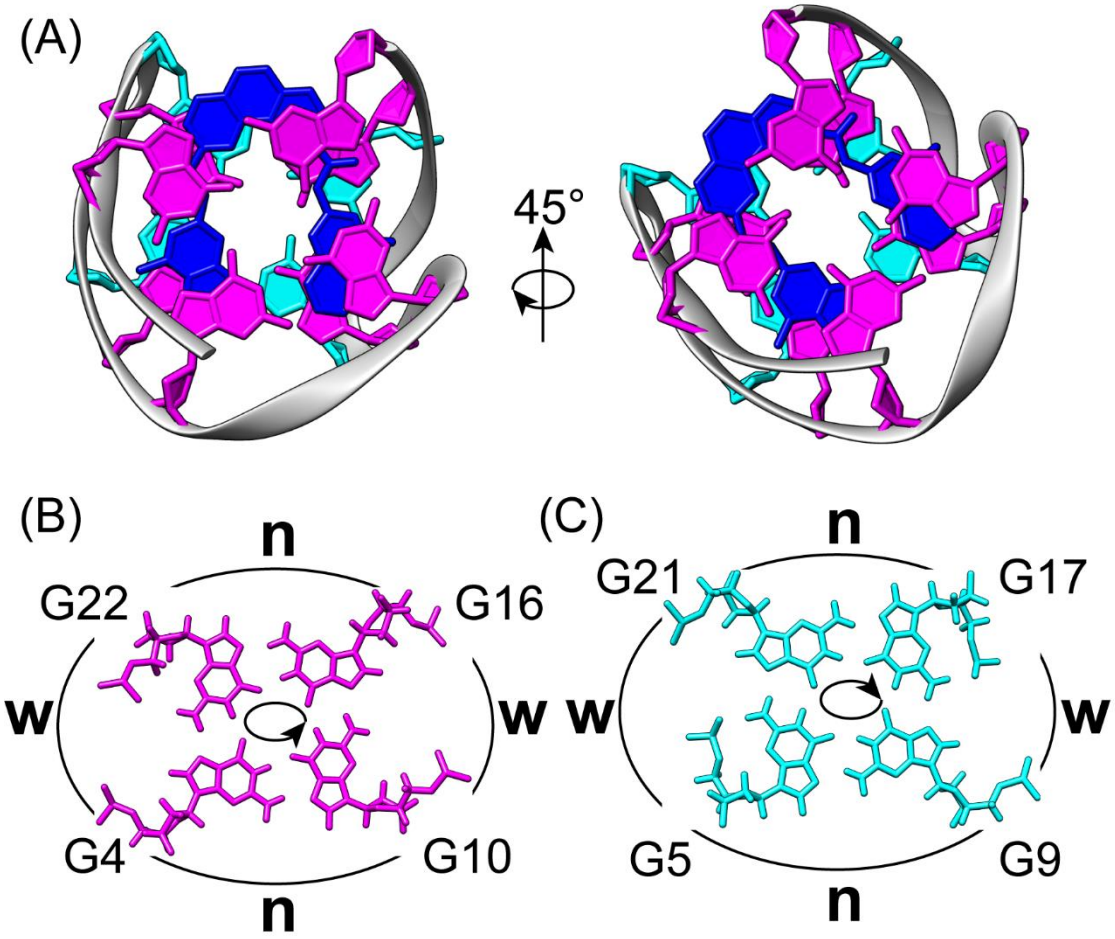

Figure S17. Representation of groove widths in 23TAG+Phen-DC$_3$ complex. (A) Representation of 23TAG+Phen-DC$_3$ complex showing the disposition of guanine quartets by magenta and cyan color. Phen-DC$_3$ is depicted in blue color. (B) G4→G10→G16→G22 quartet (magenta color) and (C) G5←G9←G17←G21 quartet (cyan color) with the description of groove widths 'nwnw' (n= narrow, w= wide). The H-bonding directionality in the quartets are shown by circular arrows in panels (B) and (C).

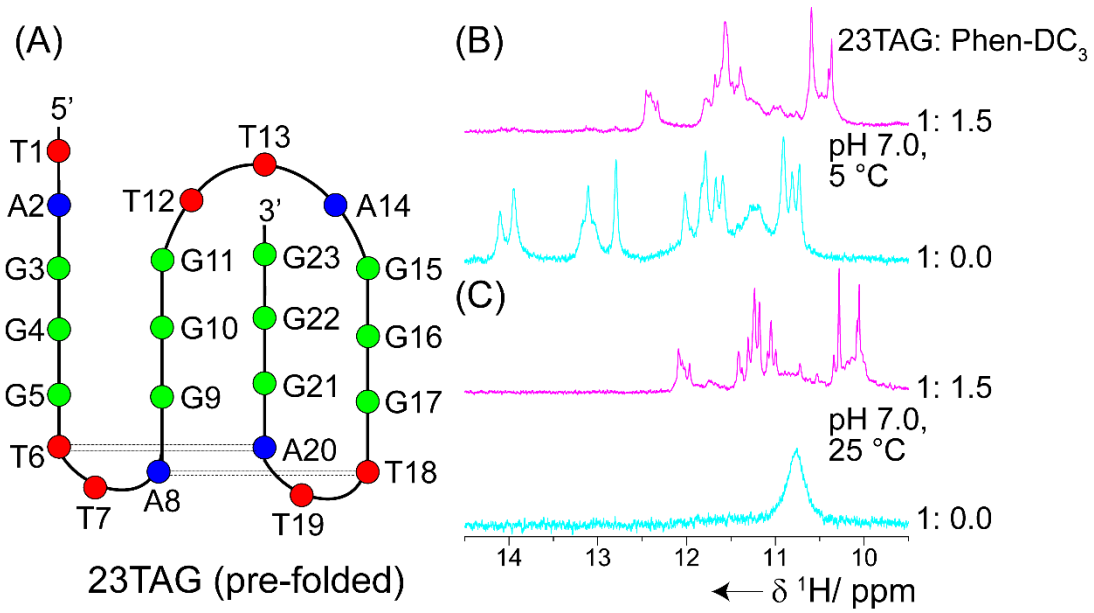

Figure S18. Phen-DC$_3$-induced conformational change of pre-folded 23TAG. (A) Schematic representation of pre-folded conformation of 23TAG in the absence of added K^+ or Na^+ cations at pH 7.[15] Guanine, adenine and thymine residues are represented as green, blue and red circles, respectively, while dashed lines represent A•T base pairs. (B) and (C) show the imino regions of the ^{1}H NMR spectra of 100 µM 23TAG at (B) 5 °C and (C) 25 °C exhibiting signals corresponding to the G4 pre-folded state (cyan) and to the complex formed upon binding of Phen-DC$_3$ at 1:1.5 mole equivalent (magenta). The ^{1}H NMR spectra were recorded on a 600 MHz NMR spectrometer in 95% H_2O/5% ^2H_2O in absence of cations promoting G4 formation.

References

[1] A. De Cian, E. DeLemos, J.-L. Mergny, M.-P. Teulade-Fichou, D. Monchaud, *J. Am. Chem. Soc.* **2007**, *129*, 1856–1857.

[2] V. Gabelica, S. Livet, F. Rosu, *J. Am. Soc. Mass Spectrom.* **2018**, *29*, 2189–2198.

[3] A. Ghosh, E. Largy, V. Gabelica, *Nucleic Acids Res.* **2021**, *49*, 2333–2345.

[4] A. T. Phan, D. J. Patel, *J. Am. Chem. Soc.* **2002**, *124*, 1160–1161.

[5] W. Lee, M. Tonelli, J. L. Markley, *Bioinformatics* **2015**, *31*, 1325–1327.

[6] I. Ivani, P. D. Dans, A. Noy, A. Pérez, I. Faustino, A. Hospital, J. Walther, P. Andrio, R. Goñi, A. Balaceanu, G. Portella, F. Battistini, J. L. Gelpí, C. González, M. Vendruscolo, C. A. Laughton, S. A. Harris, D. A. Case, M. Orozco, *Nat. Methods* **2016**, *13*, 55–58.

[7] A. Onufriev, D. Bashford, D. A. Case, *J. Phys. Chem. B* **2000**, *104*, 3712–3720.

[8] A. Pérez, I. Marchán, D. Svozil, J. Sponer, T. E. Cheatham, C. A. Laughton, M. Orozco, *Biophys. J.* **2007**, *92*, 3817–3829.

[9] M. Zgarbová, F. J. Luque, J. Šponer, T. E. Cheatham, M. Otyepka, P. Jurečka, *J. Chem. Theory Comput.* **2013**, *9*, 2339–2354.

[10] E. Vanquelef, S. Simon, G. Marquant, E. Garcia, G. Klimerak, J. C. Delepine, P. Cieplak, F.-Y. Dupradeau, *Nucleic Acids Res.* **2011**, *39*, W511–W517.

[11] W. J. Chung, B. Heddi, F. Hamon, M.-P. Teulade-Fichou, A. T. Phan, *Angew. Chem. Int. Ed.* **2014**, *53*, 999–1002; *Angew. Chem.* **2014**, *126*, 1017–1020.

[12] J. Dickerhoff, J. Dai, D. Yang, *Nucleic Acids Res.* **2021**, *49*, 5905–5915.

[13] A. T. Phan, V. Kuryavyi, K. N. Luu, D. J. Patel, *Nucleic Acids Res.* **2007**, *35*, 6517–6525.

[14] E. F. Pettersen, T. D. Goddard, C. C. Huang, G. S. Couch, D. M. Greenblatt, E. C. Meng, T. E. Ferrin, *J. Comput. Chem.* **2004**, *25*, 1605–1612.

[15] T. Frelih, B. Wang, J. Plavec, P. Šket, *Nucleic Acids Res.* **2020**, *48*, 2189–2197.